


Readout-Segmented Echo-Planar Diffusion-Weighted MR Imaging Improves the Differentiation of Breast Cancer Receptor Statuses Compared With Conventional Diffusion-Weighted Imaging

Minghao Zhong, BD,¹ Zhiqi Yang, MD,^{1,2*}  Xiaofeng Chen, MD,^{1,2*} Ruibin Huang, MD,³ Mengzhu Wang, PhD,⁴ Weixiong Fan, BD,¹ Zhuozhi Dai, PhD,^{5*} and Xiangguang Chen, MD^{1,2*}

Background: Readout-segmented echo-planar diffusion-weighted imaging (RS-EPI) can improve image quality and signal-to-noise ratio, the resulting apparent diffusion coefficient (ADC) value acts as a more sensitive biomarker to characterize tumors. However, data regarding the differentiation of breast cancer (BC) receptor statuses using RS-EPI are limited.

Purpose: To determine whether RS-EPI improves the differentiation of receptor statuses compared with conventional single-shot (SS) EPI in breast MRI.

Study Type: Retrospective.

Population: A total of 151 BC women with the mean age of 50.6 years.

Field strength/Sequence: A 3 T/ RS-EPI and SS-EPI.

Assessment: The ADCs of the lesion and normal background tissue from the two sequences were collected by two radiologists with 15 years of experience working of breast MRI (M.H.Z. and X.F.C.), and a normalized ADC was calculated by dividing the mean ADC value of the lesion by the mean ADC value of the normal background tissue.

Statistical Tests: Agreement between the ADC measurements from the two sequences was assessed using the Pearson correlation coefficient and Bland–Altman plots. One-way analysis of variance, Kruskal–Wallis test, and median difference were used to compare the ADC measurements for all lesions and different receptor statuses. A *P* value less than 0.05 indicated a significant result.

Results: The ADC measurements of all lesions and normal background tissues were significantly higher on RS-EPI than on SS-EPI (1.82 ± 0.33 vs. 1.55 ± 0.30 and 0.83 ± 0.11 vs. 0.79 ± 0.10). The normalized ADC was lower on RS-EPI than on SS-EPI (0.47 ± 0.11 vs. 0.53 ± 0.12 , a median difference of -0.04 [95% CI: -0.256 to 0.111]). For both diffusion methods, only the ADC measurement of RS-EPI was higher for human epidermal growth factor receptor-2 (HER-2)-positive tumors than for HER-2-negative tumors (0.87 ± 0.10 vs. 0.81 ± 0.11), and this measurement was associated with HER-2 positive status (adjusted odds ratio [OR] = 654.4); however, similar results were not observed for the ADC measurement of SS-EPI (0.80 ± 0.10 vs. 0.78 ± 0.11 with *P* = 0.199 and adjusted OR = 0.21 with *P* = 0.464, respectively).

View this article online at wileyonlinelibrary.com. DOI: 10.1002/jmri.28065

Received Oct 20, 2021, Accepted for publication Jan 5, 2022.

*Address reprint requests to: Z.Y., Department of Radiology, Meizhou People's Hospital, Meizhou 514031, China. E-mail: y13643090854@163.com, X.C., Department of Radiology, Meizhou People's Hospital, Meizhou 514031, China. E-mail: 15766214509@163.com, Z.D., Department of Radiology, Shantou Central Hospital, Shantou, Guangdong 515041, China. E-mail: zzdai@stu.edu.cn, or X.C., Department of Radiology, Meizhou People's Hospital, Meizhou 514031, China. E-mail: cxg966504@163.com

Minghao Zhong, Zhiqi Yang, Xiaofeng Chen, and Ruibin Huang contributed equally to the work.

From the ¹Department of Radiology, Meizhou People's Hospital, Meizhou, 514031, China; ²Guangdong Provincial Key Laboratory of Precision Medicine and Clinical Translational Research of Hakka Population, Meizhou, 514031, China; ³Department of Radiology, First Affiliated Hospital of Shantou University Medical College, Shantou, 515000, China; ⁴MR Scientific Marketing, Siemens Healthineers, Guangzhou, 510620, China; and ⁵Department of Radiology, Shantou Central Hospital, Shantou, Guangdong, 515041, China

Additional supporting information may be found in the online version of this article

This is an open access article under the terms of the [Creative Commons Attribution-NonCommercial-NoDerivs](https://creativecommons.org/licenses/by-nc-nd/4.0/) License, which permits use and distribution in any medium, provided the original work is properly cited, the use is non-commercial and no modifications or adaptations are made.

Data Conclusion: RS-EPI can improve the distinction between HER-2-positive and HER-2-negative breast cancer, complementing the clinical application of diffusion imaging.

Evidence Level: 3

Technical Efficacy: Stage 1

J. MAGN. RESON. IMAGING 2022;56:691–699.

Diffusion-weighted imaging (DWI), which is a complementary technique for dynamic contrast-enhanced (DCE) magnetic resonance imaging (MRI) that reduces false-positive rates in characterizing tumor lesions, is widely used in breast imaging and plays a useful role in the diagnosis, treatment, and prognosis of breast cancer (BC).^{1–8} Apparent diffusion coefficient (ADC) maps obtained with DWI can provide information about the microscopic cellular environment that can be used for characterizing tumors.^{7,9,10}

A major strength of the ADC is its quantitative character, which allows it to be used as a potential imaging biomarker for characterizing prognostic factors, such as estrogen receptor (ER), progesterone receptor (PR), and human epidermal growth factor receptor-2 (HER-2) expression, as well as the proliferation rate (Ki-67).^{3,11} Numerous studies have shown that tumors with a high Ki-67 index and an increased cell density are expected to have lower ADC measurements than tumors with a low Ki-67 index, whereas HER-2-positive tumors with increased neovascularity are expected to have higher ADC measurements than HER2-negative tumors, and similar results have been observed when comparing hormone receptor-positive tumors with hormone receptor-negative tumors.^{3,12–15}

However, previous studies have reached inconsistent results in using ADC to identify these prognostic factors.^{16–18} These disagreements might be attributable to the use of different MRI techniques. For example, readout-segmented (RS) echo-planar diffusion-weighted imaging (EPI) based on segment sampling of the EPI sequence in the readout direction can improve image quality and signal-to-noise ratio (SNR), and the resulting ADC value acts as a more sensitive imaging biomarker to predict BC receptor statuses than the ADC from single-shot (SS) EPI.^{3,16–19} However, there are still limited data regarding the diagnostic performance of RS-EPI and its potential to replace SS-EPI in characterizing the receptor statuses of BC. Therefore, this study aimed to compare the sensitivity and reliability of RS-EPI in the characterization of receptor statuses in clinical practice with those of SS-EPI.

Materials and Methods

Patients

This single-center retrospective study was approved by the institutional review board, and the requirement for patient informed consent was waived. This study retrospectively collected data from 316 consecutive breast cancer women with invasive ductal carcinoma (IDC) and age range of 25–81 years who underwent both RS-EPI and conventional SS-EPI preoperatively between January 2016 and October 2018. The

exclusion criteria were as follows: 1) 60 patients without surgery (mastectomy or breast conserving) were excluded because the biopsy and surgical specimens may have different results in receptor statuses and Ki-67 proliferation. The pathological results of surgery were used as the standard, 2) 92 patients who had received neoadjuvant chemotherapy before surgery were excluded since the tumor characteristics might be changed during neoadjuvant chemotherapy, (3) four patients with a previous history of BC, and (4) nine patients with poor image quality or no lesion visibility on the MRI images decided by two radiologists (M.H.Z. and X.F.C.). Finally, 151 patients were included in the study, and the mean age of the patients was 50.6 ± 10.7 years (range: 25–81 years). Out of all patients, 74 patients were premenopause and 77 patients were postmenopause.

Clinical Data

Clinicopathological data, including age, maximum and minimum tumor diameter, ER, PR, and HER-2 statuses, and Ki-67 index, were obtained from the medical electronic record system. The tumor size was measured on the largest section of the BC in the DCE-MRI images. ER- or PR-positive tumors were defined as tumors with at least 1% of cells that were positively stained according to immunohistochemistry.^{2,20} HER-2-positive tumors were defined as tumors with scores of 3+ or tumors with scores of 2+ and positive fluorescence in situ hybridization results of HER-2 gene amplification.²¹ A Ki-67 index $\geq 20\%$ indicated high expression.^{2,20}

MRI Techniques

All the examinations were performed on a 3 T MRI scanner (MAGNETOM Skyra, Siemens Healthcare, Erlangen, Germany) with a 16-channel bilateral breast coil using prone positioning. The scanning protocol included conventional T₁-weighted acquisition (repetition time [TR]/echo time [TE] 5.5/2.5 msec, field of view [FOV] 341 mm \times 341 mm, matrix 426 \times 448, slice thickness 1.5 mm, slice gap 0.3 mm), T₂-weighted acquisition (TR/TE 3570/74 msec, inversion time 230 msec, FOV 341 mm \times 341 mm, matrix 314 \times 448, slice thickness 4.0 mm, slice gap 0.4 mm), DWI, and a DCE series. The DCE series consisted of precontrast T₁-weighted volume interpolated breath-hold examination (VIBE) imaging (TR/TE 3.78/1.38 msec, FOV 340 mm \times 340 mm, matrix 205 \times 256, slice thickness 2 mm, voxel resolution 1.3 mm \times 1.3 mm \times 2.0 mm) and multi arterial time-resolved imaging with interleaved stochastic trajectories (TWIST)-VIBE DCE scanning with 34 consecutive phases (TR/TE 6.4/ 3.34 msec, slice thickness 2.0 mm, FOV 340 mm \times 340 mm, matrix 289 \times 303, temporal resolution 8.9 seconds) after intravenous bolus injection of gadopentetate dimeglumine (Bayer Pharma AG) with an injection rate of 3.0 mL/sec.

Axial DWI images were sequentially obtained by RS-EPI and SS-EPI techniques before contrast enhancement. RS-EPI and SS-EPI sequences were designed with the same b-values (50 and 800 sec/mm²) in-plane resolution of 1.8 \times 1.8 mm², a slice thickness of 4.0 mm with

TABLE 1. The Clinical and Imaging Features of Breast Cancer Patients With Invasive Ductal Carcinoma

Receptor Status	Age (year)	Maximum Diameter	Minimum Diameter	ADC Value of RS-EPI ($\times 10^{-3} \text{ cm}^2$)	ADC Value of SS-EPI ($\times 10^{-3} \text{ cm}^2$)	Normalized ADC Value of RS-EPI	Normalized ADC Value of SS-EPI
ER							
Negative (n = 56)	51.59 ± 9.07	4.01 ± 1.67	2.58 ± 1.12	0.84 ± 0.12	0.80 ± 0.10	0.46 ± 0.11	0.52 ± 0.13
Positive (n = 95)	50.01 ± 11.62	3.30 ± 1.69	2.02 ± 0.92	0.83 ± 0.11	0.78 ± 0.10	0.48 ± 0.11	0.53 ± 0.12
<i>P</i> value	0.385	0.002	<0.001	0.510	0.480	0.543	0.282
PR							
Negative (n = 92)	52.33 ± 10.31	3.86 ± 1.86	2.46 ± 1.10	0.82 ± 0.11	0.78 ± 0.11	0.46 ± 0.11	0.51 ± 0.13
Positive (n = 59)	47.90 ± 10.93	3.10 ± 1.35	1.85 ± 0.80	0.85 ± 0.11	0.80 ± 0.10	0.50 ± 0.11	0.56 ± 0.11
<i>P</i> -value	0.013	0.006	<0.001	0.192	0.480	0.020	0.002
HER-2							
Negative (n = 100)	51.00 ± 11.25	3.43 ± 1.68	2.20 ± 1.08	0.81 ± 0.11	0.78 ± 0.11	0.46 ± 0.11	0.52 ± 0.12
Positive (n = 51)	49.90 ± 9.75	3.82 ± 1.76	2.27 ± 0.93	0.87 ± 0.10	0.80 ± 0.10	0.51 ± 0.11	0.55 ± 0.13
<i>P</i> value	0.572	0.204	0.365	0.001	0.199	0.010	0.173
Ki-67							
<20% (n = 36)	51.44 ± 10.63	3.18 ± 1.22	1.80 ± 0.60	0.84 ± 0.11	0.80 ± 0.11	0.50 ± 0.10	0.55 ± 0.12
≥20% (n = 115)	50.33 ± 10.81	3.68 ± 1.83	2.36 ± 1.10	0.83 ± 0.12	0.79 ± 0.10	0.46 ± 0.11	0.52 ± 0.12
<i>P</i> value	0.589	0.210	0.003	0.398	0.551	0.029	0.154

Bold values indicate statistically significant in *P* values.
 ER = estrogen receptor; PR = progesterone receptor; HER-2 = human epidermal growth factor receptor-2; ADC = apparent diffusion coefficient.

a slice gap of 0.8 mm, generalized auto-calibrating partially parallel acquisitions (GRAPPAs) was also used in both sequences with an acceleration factor of 2, and enough slices were acquired to cover the entire breast. In order to match the total acquisition time of the two sequences (approximately 5 minutes), the number of averages for SS-EPI and RS-EPI was set to 8 and 3, respectively. The RS-EPI sequence used five readout segments. The remainder of the parameters were as follows: RS-EPI (TR/TE 4800/56 msec, FOV 170 mm × 340 mm, bandwidth 822 Hz, matrix 98 × 190, echo spacing 0.36 msec) and SS-EPI (TR/TE 4200/62 ms,ec FOV 149 mm × 340 mm, bandwidth 1730 Hz, matrix 100 × 170, echo spacing 0.68 msec).

MRI Image Analysis

All the imaging analyses were independently carried out by two radiologists with 15 years of experience working with breast MRI (M.H. Z. and X.F.C.). All the image data were transferred to a Siemensyngo.via workstation. The BCs were identified on high b-value (800 sec/mm²) images using DCE-MR images for reference and then evaluated on ADC maps using breast Tissue 4D software package embedded in dedicated workstation (Syngo.via).

The representative slice of the lesion that showed the largest section of the tumor was identified by the radiologist, and a freehand region of interest (ROI) with a size range of 20–30 mm² was drawn on the lowest hypointensity region of the lesion on the RS-EPI maps corresponding to a prominent area of enhancement on the DCE-MRI images. The ROI was placed to avoid visibly necrotic, cystic, bleeding, and calcification areas. Then the same ROI was copied to SS-EPI maps to measure the ADC value of tumor. For the ADC measurement of normal background tissue, the same ROI was copied to RS-EPI maps and SS-EPI maps on contralateral normal breast tissue. The corresponding ADC values of each lesion and the normal background tissue from RS-EPI and SS-EPI were recorded after motion correction. Each ADC value (×10⁻³ mm²) was measured three times, which were located on the largest tumor section and its adjacent sections, and then the averaged value was calculated for further analysis.

To reduce the impact of individual breast characteristics, normalized ADC (nADC) was introduced and calculated as the mean ADC value of the lesion divided by the mean ADC value of the normal background tissue.^{6,22}

Statistical Analysis

Statistical analysis was performed using R (Version 4.0.3, RFoundation for Statistical Computing, Vienna, Austria). Continuous variables are expressed as the mean ± standard deviation. Categorical variables are expressed as counts (percentages). The normality of the variables was investigated by using the Shapiro–Wilk test. For normally distributed variables, one-way analysis of variance was used to assess the difference between the RS-EPI measurement and the SS-EPI measurement in different receptor statuses, while the Kruskal–Wallis test was used for non-normally distributed variables.

Univariate and multivariate logistic regression models were fitted and used to identify the risk factors for predictive positive receptor statuses. In addition, a paired *t*-test (for normally distributed variables) or a paired Wilcoxon test was used to compare the ADC measurement from RS-EPI and SS-EPI for all lesions and different receptor statuses. The median difference (assumed symmetric distribution) between RS-EPI and SS-EPI measurements, subtracting

TABLE 2. Univariate and Multivariate Analysis of the Parameters of Different Receptor Statuses

	PR			HER-2			Ki-67													
	Univariate Analysis		Multivariate Analysis	Univariate Analysis		Multivariate Analysis	Univariate Analysis		Multivariate Analysis											
	OR	P	Cutoff	OR	P	Cutoff	OR	P	Cutoff											
Age	0.99	0.383	39.50	0.98	0.304	0.96	0.015	49.50	0.96	0.017	0.99	0.570	55.50	1.00	0.868	0.99	0.586	50.50	0.99	0.412
Max-diameter	0.78	0.016	2.55	0.92	0.524	0.74	0.010	2.65	0.91	0.545	1.140	0.193	3.45	1.17	0.251	1.22	0.130	2.55	0.87	0.398
Min-diameter	0.57	0.003	2.21	0.62	0.043	0.42	0.001	1.65	0.46	0.019	1.07	0.678	2.65	0.99	0.959	2.33	0.006	2.26	2.86	0.008
ADC value of RS-EPI	0.37	0.508	0.86	0.19	0.391	7.08	0.191	0.93	1.97	0.728	240.7	0.001	0.76	654.4	0.002	0.24	0.396	0.94	0.88	0.953
ADC value of SS-EPI	0.31	0.478	0.767	0.82	0.92	3.20	0.472	0.78	1.80	0.784	8.83	0.200	0.65	0.21	0.464	0.22	0.421	0.70	0.13	0.401

Bold values indicate statistically significant in *P* values.
 Max = maximum; Min = Minimum; OR = odds ratio; ER = estrogen receptor; PR = progesterone receptor; HER-2 = human epidermal growth factor receptor-2.

the SS-EPI measurement from the RS-EPI measurement, was tracked and further compared among tumors with different receptor statuses. Interobserver agreements for the RS-EPI and SS-EPI measurements between the two radiologists were assessed using the intraclass correlation coefficient (ICC), which was categorized as good agreement (0.61–0.80) and excellent agreement (≥ 0.81).²³ The agreement between the RS-EPI and SS-EPI measurements was analyzed using Pearson correlation and Bland–Altman analysis. A *P* value less than 0.05 indicated a significant result.

Results

Basic Clinicopathological Characteristics

A total of 151 IDC patients were analyzed, and their mean age was 50.6 ± 10.7 years. The table comparing measurements using average values of two readers are shown in Table 1, and the table comparing measurements using annotations of reader 1 and 2 are shown in Tables E1 and E2 in the supplementary materials. The maximum and minimum tumor diameters of ER-negative tumors were higher than those of ER-positive tumors (4.01 ± 1.67 vs. 3.29 ± 1.69 and 2.58 ± 1.12 vs. 2.02 ± 0.92 , respectively), those of PR-negative tumors were higher than those of PR-positive tumors (3.86 ± 1.86 vs. 3.10 ± 1.35 and 2.46 ± 1.10 vs. 1.85 ± 0.80 , respectively). However, the minimum diameter of low Ki-67 index tumors was smaller than that of high Ki-67 index tumors (1.80 ± 0.60 vs. 2.36 ± 1.10). In addition, the age of PR-positive patients was younger than that of PR-negative patients (47.90 ± 10.93 vs. 52.33 ± 10.31).

Comparisons of the ADC Measurement of Tumors With Different Receptor Statuses

The ADC measurements from RS-EPI were significantly higher for HER-2-negative tumors than for HER-2-positive tumors (0.81 ± 0.11 vs. 0.87 ± 0.10), but this difference was not confirmed with the ADC measurements of SS-EPI (0.78 ± 0.11 vs. 0.80 ± 0.10 , *P* = 0.199). In addition, there was no significant difference in the ADC measurements from RS-EPI and SS-EPI with respect to the other receptor statuses or the Ki-67 index (Table 1). Paired comparisons of the ADC measurements of tumors with different receptor statuses using univariate and multivariate analysis revealed (Table 2) that a younger age (<49.5 years, adjusted odds ratio [OR] = 0.96) and a lower minimum diameter (<1.65 cm, adjusted OR = 0.46) were associated with PR-positive status, while higher ADC measurements from RS-EPI ($>0.76 \times 10^{-3}$ mm², adjusted OR = 654.4) were associated with HER2-positive status. Representative ADC images of RS-EPI and SS-EPI sequences from a breast cancer patient with HER-2-negative and HER-2-positive invasive ductal carcinoma are shown in Fig. 1.

Interobserver Agreement

The ICC values for the ADC measurements from RS-EPI and SS-EPI between the two radiologists were 0.657 (95% CI: 0.543–0.748) and 0.740 (95% CI: 0.647–0.811), respectively, indicating good agreement. The Bland–Altman plots of ADC measurement of SS-EPI and RS-EPI from two

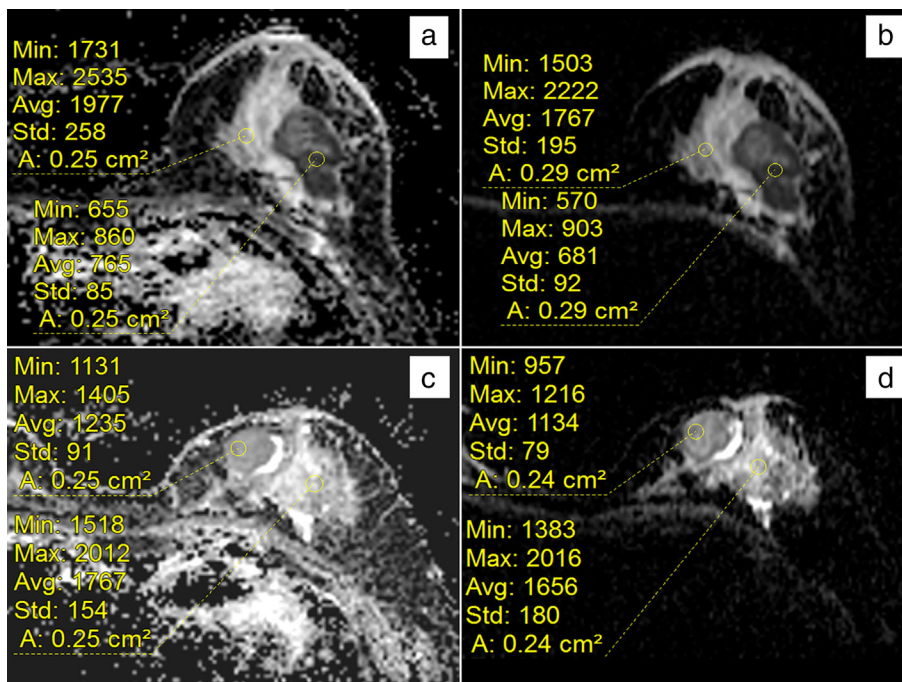


FIGURE 1: Representative ADC images of RS-EPI and SS-EPI sequences from a breast cancer patient with HER-2-negative and HER-2-positive invasive ductal carcinoma; (a) and (b) are HER-2-negative images of a left breast invasive ductal carcinoma patient. Measuring the ADC map revealed a mean ADC value of 0.765×10^{-3} mm²/sec by RS-EPI (a) and 0.681×10^{-3} mm²/sec by SS-EPI (b); (c) and (d) are images of a HER-2-positive left breast invasive ductal carcinoma patient. Measuring the ADC map revealed a mean ADC value of 1.235×10^{-3} mm²/sec by RS-EPI (c) and 1.134×10^{-3} mm²/sec by SS-EPI (d).

TABLE 3. Comparison of ADC Values From RS-EPI and SS-EPI for Tumors With Different Receptor Statuses

	ADC Value of RS-EPI ($\times 10^{-3} \text{ cm}^2$)	ADC Value of SS-EPI ($\times 10^{-3} \text{ cm}^2$)	P^a	Median Difference (95% CI)	P^b
ER					0.824
Negative ($n = 56$)	0.84 ± 0.12	0.80 ± 0.10	0.056	0.026 (−0.106 to 0.294)	
Positive ($n = 95$)	0.83 ± 0.11	0.78 ± 0.10	0.008	0.041 (−0.135 to 0.255)	
PR					0.587
Negative ($n = 92$)	0.82 ± 0.11	0.78 ± 0.11	0.027	0.031 (−0.122 to 0.244)	
Positive ($n = 59$)	0.85 ± 0.11	0.80 ± 0.10	0.023	0.052 (−0.13 to 0.264)	
HER2					0.012
Negative ($n = 100$)	0.81 ± 0.11	0.78 ± 0.10	0.082	0.022 (−0.121 to 0.249)	
Positive ($n = 51$)	0.87 ± 0.10	0.80 ± 0.10	0.001	0.059 (−0.133 to 0.312)	
Ki-67					0.656
<20% ($n = 36$)	0.84 ± 0.11	0.80 ± 0.11	0.096	0.054 (−0.132 to 0.217)	
$\geq 20\%$ ($n = 115$)	0.83 ± 0.12	0.79 ± 0.10	0.017	0.036 (−0.126 to 0.26)	

P^a indicates the comparison of ADC measurements between RS-EPI and SS-EPI and P^b indicates the comparison of ADC measurements for tumors with different receptor statuses. RS-EPI and SS-EPI indicate the ADC measurements of the RS-EPI and SS-EPI sequences, respectively. Bold values indicate statistically significant in P values. ER = estrogen receptor; PR = progesterone receptor; HER-2 = human epidermal growth factor receptor-2.

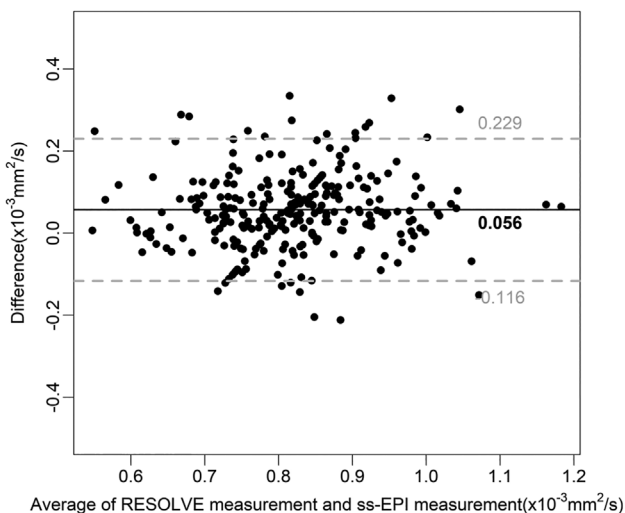


FIGURE 2: Bland-Altman plots showing the agreement between the RS-EPI measurement and the SS-EPI measurement for all lesions. Solid horizontal lines represent the mean bias, and the top and bottom dashed lines denote the upper and lower limits of agreement, respectively.

radiologists for all lesions are shown in Fig. E1 in the supplementary materials. In addition, the ICC values for the maximum diameter and minimum diameter of tumor between the two radiologists were 0.963 (95% CI: 0.949–0.973) and 0.945 (95% CI: 0.925–0.960), respectively.

Agreement Between ADC Measurements: RS-EPI vs. SS-EPI

There was a moderate positive correlation between the ADC measurements from RS-EPI and SS-EPI ($r = 0.679$; 95% CI: 0.613–0.73) for all lesions. However, the mean ADC measurements from RS-EPI for all lesions were higher than the mean ADC measurements of SS-EPI (0.83 ± 0.11 vs. 0.79 ± 0.10). These differences remained significant for ER-positive tumors (0.83 ± 0.11 vs. 0.78 ± 0.10), PR-positive tumors (0.82 ± 0.11 vs. 0.78 ± 0.11), PR-negative tumors (0.85 ± 0.11 vs. 0.80 ± 0.10), HER-2-positive tumors (0.87 ± 0.10 vs. 0.80 ± 0.10), and tumors with a high Ki-67 index (0.83 ± 0.12 vs. 0.79 ± 0.10) (Table 3).

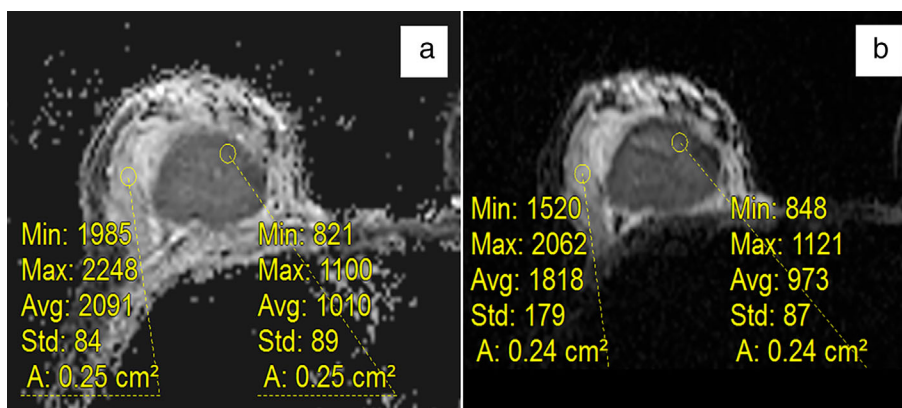


FIGURE 3: Representative ADC images of normal background tissue and normalized ADC on RS-EPI and SS-EPI maps. The mean ADC value of the normal background tissue was $2.091 \times 10^{-3} \text{ mm}^2/\text{sec}$ in the RS-EPI maps (a) and $1.818 \times 10^{-3} \text{ mm}^2/\text{sec}$ in the SS-EPI maps (b). The normalized ADC was 0.48 for RS-EPI and 0.54 for SS-EPI.

To further explore the differences between the RS-EPI and SS-EPI measurements for different receptor statuses, the median difference in the ADC measurements for tumors with different receptor statuses only revealed a significant difference between HER-2-negative and HER-2-positive tumor, with a higher difference between RS-EPI and SS-EPI measurements for HER-2-positive tumors than for HER-2-negative tumors (0.059 [95% CI: -0.133 to 0.312] vs. 0.022 [95% CI: -0.121 to 0.249]). Bland–Altman plots showed a mean bias of $0.056 \times 10^{-3} \text{ mm}^2/\text{sec}$ (lower than the upper limit of agreement, -0.12 to 0.23) for all lesions between the ADC measurements from RS-EPI and SS-EPI (Fig. 2).

Comparison of the Normalized ADC: RS-EPI vs. SS-EPI

RS-EPI yielded significantly higher ADC measurements of normal background tissue than SS-EPI (1.82 ± 0.33 vs. 1.55 ± 0.30). However, the normalized ADC was significantly lower on RS-EPI than on SS-EPI (0.47 ± 0.11 vs. 0.53 ± 0.12). Further analysis showed that the median difference in the normalized ADC between RS-EPI and SS-EPI revealed a significant difference between the two sequences, favoring a lower normalized ADC by using RS-EPI (-0.04 [95% CI: -0.256 to 0.111]). Representative ADC images of the normal background tissue and the normalized ADC in the RS-EPI and SS-EPI maps are shown in Fig. 3. In addition, the normalized ADC value of RS-EPI were lower for PR-negative tumors than for PR-positive tumors (0.46 ± 0.11 vs. 0.50 ± 0.11), and this difference was confirmed with the normalized ADC value of SS-EPI (0.51 ± 0.13 vs. 0.56 ± 0.11). The normalized ADC value of RS-EPI was lower for HER-2-negative tumors than for HER-2-positive tumors (0.46 ± 0.11 vs. 0.51 ± 0.11) and lower for high Ki-67 index tumors than for low Ki-67 index tumors (0.46 ± 0.11 vs. 0.50 ± 0.10), but those differences were not detectable with the normalized ADC value of SS-EPI (0.52 ± 0.12 vs.

0.55 ± 0.13 with $P = 0.173$, and 0.52 ± 0.12 vs. 0.55 ± 0.12 with $P = 0.154$, respectively) (Table 1).

Discussion

The ADC measurements from RS-EPI and SS-EPI of BC patients were assessed in this study. Compared to SS-EPI, RS-EPI has the potential advantage of differentiating between breast lesions with different receptor statuses. The results demonstrate that higher ADC measurements from RS-EPI are associated with HER2-positive status, which improves the diagnosis of HER-2 status in BC. In terms of hormone receptor statuses, although the ADC values were not significantly different, there were significant differences in tumor diameter.

It is well known that the ADC value correlates with tumor grade and proliferation index; however, previous research reported that there were no statistically significant associations between ADC values and breast cancer receptor statuses.^{24–28} This study indicates that the solution may be to use RS-EPI. This study found that the ADC value from RS-EPI could distinguish between HER-2-positive and HER-2-negative tumors, which cannot be achieved using the ADC value from traditional SS-EPI. According to the previous literature, the RS-EPI technique can better visualize anatomical details, and it results in a higher image quality than SS-EPI by reducing image distortion and improving the spatial resolution with two-dimensional navigator echoes using shortened echo spacing.^{8,29,30} In RS-EPI sequence, this shortened k-space traversal in the phase encoding direction results in less attenuation of T2* during readout, which leads to a reduction in distortion and blurring.³¹ Although these segmentations in RS-EPI increase the scanning time, the accompanying shorter echo time increases imaging signal level. Moreover, the motion-induced phase errors were corrected by 2D navigator echoes technique in RS-EPI (Fig. E2 was added to the supplementary material to demonstrate the image quality of RS-EPI and SS-EPI). Amornsiripanitch et al indicated that using RS-EPI was more sensitive than using SS-

EPI to detect BC.³² Bogner et al also demonstrated that ADC measurements from RS-EPI could improve the distinction of benign from malignant lesions.²⁹

Similar to the finding in gastric cancers, the ADC values were higher in HER-2-positive tumors.³³ HER-2 is a prognostic and predictive biomarker in several human cancers.³⁴ The over expression of HER-2 enables the activation of growth signaling pathways to promote cell proliferation and suppress apoptosis; therefore, HER-2 positivity is associated with malignant tumors. According to previous studies, malignant lesions generally exhibit lower ADC measurements than benign lesions but with a significant overlap.^{6,14,35} However, this study showed that HER-2-positive tumors exhibited higher ADC measurements than HER-2-negative tumors. A potential explanation for this result may be that HER-2-positive tumors have increased tumor angiogenesis and perfusion, resulting in higher ADC measurements *in vivo*.¹⁴

Although ADC values are not significantly different in tumors with different hormone receptor (ER and PR) statuses, there are significant differences in tumor diameter, but of which is not a DWI-specific feature. Consistent with previous research, larger tumors were more likely to be ER- and PR-negative, indicating the potential advanced stage of the tumor.^{36,37} Moreover, a larger tumor size was associated with a higher risk of recurrence.³⁸ However, the tumor diameter cannot reflect the status of HER-2 in this study.

It is worth noting that ADC measurements are confounded by multiple factors, including imaging parameters, data analysis, and pathophysiologic features.^{6,22,39} Therefore, special ADC measurement methods should be used to reduce the above variation to reliably assess its clinical utility. Similar to previous studies, ADC normalization in this study was introduced to reduce these variations.^{8,39} This study showed that the normalized ADC from RS-EPI was significantly lower than that from SS-EPI. This result is partly consistent with a previous study that showed a low normalized ADC for RS-EPI on breast MRI compared with conventional ADC, resulting in a reduction in the overlap of ADCs between benign and malignant lesions and an increase in the diagnostic performance.^{7,39}

Limitations

First, although this study was conducted with a relatively large cohort at a single institution. Findings from a larger multicenter study could make the results more reliable and provide more effective evidence of RS-EPI for diagnosis. Second, due to the time-consuming manual measurement of 3D ROIs that may better reflect the ADC measurements of tumors, 2D ROIs were only used to evaluate the tumors. 3D tumor segmentation could potentially be automated for evaluation of the entire tumor in the future. Third, the difference in ADC values between RS-EPI and SS-EPI is still unknown. Although previous research also reported this difference, further research to understand the

source of this discrepancy will be meaningful.²⁹ Fourth, this results show that ADC values of RS-EPI can only distinguish HER-2 positive and HER-2 negative tumors, which may limit its utility. In contrast, the normalized ADC values of RS-EPI have better performance in distinguishing PR, HER-2, and KI-67 status. However, it is still difficult to determine the status of ER through diffusion imaging, which requires further exploration in the future.

Conclusion

This study demonstrated that the ADC value from RS-EPI can improve the distinction between HER-2-positive and HER-2-negative breast cancer, complementing the clinical application of diffusion imaging.

Acknowledgments

This study was supported in part by grants from the National Natural Science Foundation of China (82101985) and Medical Scientific Foundation of Guangdong Province (B2021280). These funding sources had no involvement in writing the article nor in the decision to submit this work for publication. In addition, the authors thank Jiayang Song from the GE Healthcare at China for help of with data processing.

Ethics Approval and Consent to Participate

This retrospective study was approved by the institutional review board of Meizhou People's Hospital.

Consent for Publication

The institutional review board waived the need to obtain informed consent for this retrospective study.

Data Availability

The data cohorts used and/or analyzed in the present study are available from the corresponding authors upon reasonable request.

Conflict of interests

One author of the study (M.Z.W.) is a consultant for Siemens Healthcare and provided some critical technical support in the manuscript. Other authors are not employees or consultants in the industrial fields and have reported any data or information that may present a conflict of interest.

References

1. Fan WX, Chen XF, Cheng FY, et al. Retrospective analysis of the utility of multiparametric MRI for differentiating between benign and malignant breast lesions in women in China. *Medicine (Baltimore)* 2018;97:e9666.
2. Chen X, Chen X, Yang J, Li Y, Fan W, Yang Z. Combining dynamic contrast-enhanced magnetic resonance imaging and apparent diffusion coefficient maps for a radiomics nomogram to predict pathological complete response to neoadjuvant chemotherapy in breast cancer patients. *J Comput Assist Tomogr* 2020;44:275-283.

3. Horvat JV, Bernard-Davila B, Helbich TH, et al. Diffusion-weighted imaging (DWI) with apparent diffusion coefficient (ADC) mapping as a quantitative imaging biomarker for prediction of immunohistochemical receptor status, proliferation rate, and molecular subtypes of breast cancer. *J Magn Reson Imaging* 2019;50:836-846.
4. Leithner D, Moy L, Morris EA, Marino MA, Helbich TH, Pinker K. Abbreviated MRI of the breast: Does it provide value? *J Magn Reson Imaging* 2019;49:e85-e100.
5. Allarakha A, Gao Y, Jiang H, Wang PJ. Prediction and prognosis of biologically aggressive breast cancers by the combination of DWI/DCE-MRI and immunohistochemical tumor markers. *Discov Med* 2019;27:7-15.
6. Partridge SC, McDonald ES. Diffusion weighted magnetic resonance imaging of the breast: Protocol optimization, interpretation, and clinical applications. *Magn Reson Imaging Clin N Am* 2013;21:601-624.
7. Rahbar H, Partridge SC. Multiparametric MR imaging of breast cancer. *Magn Reson Imaging Clin N Am* 2016;24:223-238.
8. Wisner DJ, Rogers N, Deshpande VS, et al. High-resolution diffusion-weighted imaging for the separation of benign from malignant BI-RADS 4/5 lesions found on breast MRI at 3T. *J Magn Reson Imaging* 2014;40:674-681.
9. Yamaguchi K, Nakazono T, Egashira R, et al. Diagnostic performance of diffusion tensor imaging with readout-segmented Echo-planar imaging for invasive breast cancer: Correlation of ADC and FA with pathological prognostic markers. *Magn Reson Med Sci* 2017;16:245-252.
10. Yang ZL, Hu YQ, Huang J, et al. Detection and classification of breast lesions with readout-segmented diffusion-weighted imaging in a large Chinese cohort. *Front Oncol* 2021;11:636471.
11. Bickel H, Pinker K, Polanec S, et al. Diffusion-weighted imaging of breast lesions: Region-of-interest placement and different ADC parameters influence apparent diffusion coefficient values. *Eur Radiol* 2017;27:1883-1892.
12. Shin JK, Kim JY. Dynamic contrast-enhanced and diffusion-weighted MRI of estrogen receptor-positive invasive breast cancers: Associations between quantitative MR parameters and Ki-67 proliferation status. *J Magn Reson Imaging* 2017;45:94-102.
13. Huang Y, Lin Y, Hu W, et al. Diffusion kurtosis at 3.0T as an in vivo imaging marker for breast cancer characterization: Correlation with prognostic factors. *J Magn Reson Imaging* 2019;49:845-856.
14. Park SH, Choi HY, Hahn SY. Correlations between apparent diffusion coefficient values of invasive ductal carcinoma and pathologic factors on diffusion-weighted MRI at 3.0 tesla. *J Magn Reson Imaging* 2015;41:175-182.
15. Karan B, Pourbagher A, Torun N. Diffusion-weighted imaging and (18) F-fluorodeoxyglucose positron emission tomography/computed tomography in breast cancer: Correlation of the apparent diffusion coefficient and maximum standardized uptake values with prognostic factors. *J Magn Reson Imaging* 2016;43:1434-1444.
16. Surov A, Chang YW, Li L, et al. Apparent diffusion coefficient cannot predict molecular subtype and lymph node metastases in invasive breast cancer: A multicenter analysis. *BMC Cancer* 2019;19:1043.
17. Yuan C, Jin F, Guo X, Zhao S, Li W, Guo H. Correlation analysis of breast cancer DWI combined with DCE-MRI imaging features with molecular subtypes and prognostic factors. *J Med Syst* 2019;43:83.
18. Aydin H, Guner B, Esen Bostanci I, et al. Is there any relationship between adc values of diffusion-weighted imaging and the histopathological prognostic factors of invasive ductal carcinoma? *Br J Radiol* 2018;91:20170705.
19. Bickel H, Pinker-Domenig K, Bogner W, et al. Quantitative apparent diffusion coefficient as a noninvasive imaging biomarker for the differentiation of invasive breast cancer and ductal carcinoma in situ. *Invest Radiol* 2015;50:95-100.
20. Yang Z, Chen X, Zhang T, et al. Quantitative multiparametric MRI as an imaging biomarker for the prediction of breast cancer receptor status and molecular subtypes. *Front Oncol* 2021;11:628824.
21. Liu Z, Li R, Liang K, et al. Value of digital mammography in predicting lymphovascular invasion of breast cancer. *BMC Cancer* 2020;20:274.
22. Nguyen VT, Rahbar H, Olson ML, Liu CL, Lehman CD, Partridge SC. Diffusion-weighted imaging: Effects of intravascular contrast agents on apparent diffusion coefficient measures of breast malignancies at 3 tesla. *J Magn Reson Imaging* 2015;42:788-800.
23. Landis JR, Koch GG. The measurement of observer agreement for categorical data. *Biometrics* 1977;33:159-174.
24. Baltzer P, Mann RM, Lima M, et al. Diffusion-weighted imaging of the breast-a consensus and mission statement from the EUSOBI international breast diffusion-weighted imaging working group. *Eur Radiol* 2020;30:1436-1450.
25. Zhang Y, Zhu Y, Zhang K, et al. Invasive ductal breast cancer: Preoperative predict Ki-67 index based on radiomics of ADC maps. *Radiol Med* 2020;125:109-116.
26. Newitt DC, Amouzandeh G, Partridge SC, et al. Repeatability and reproducibility of ADC histogram metrics from the ACRIN 6698 breast cancer therapy response trial. *Tomography (Ann Arbor, Mich)* 2020;6:177-185.
27. Amornsiripanitch N, Nguyen VT, Rahbar H, et al. Diffusion-weighted MRI characteristics associated with prognostic pathological factors and recurrence risk in invasive ER+/HER2- breast cancers. *J Magn Reson Imaging* 2018;48:226-236.
28. Costantini M, Belli P, Distefano D, et al. Magnetic resonance imaging features in triple-negative breast cancer: Comparison with luminal and HER2-overexpressing tumors. *Clin Breast Cancer* 2012;12:331-339.
29. Bogner W, Pinker-Domenig K, Bickel H, et al. Readout-segmented echo-planar imaging improves the diagnostic performance of diffusion-weighted MR breast examinations at 3.0 T. *Radiology* 2012;263:64-76.
30. Singer L, Wilmes LJ, Saritas EU, et al. High-resolution diffusion-weighted magnetic resonance imaging in patients with locally advanced breast cancer. *Acad Radiol* 2012;19:526-534.
31. Kim YJ, Kim SH, Kang BJ, et al. Readout-segmented echo-planar imaging in diffusion-weighted mr imaging in breast cancer: Comparison with single-shot echo-planar imaging in image quality. *Korean J Radiol* 2014;15:403-410.
32. Amornsiripanitch N, Bickelhaupt S, Shin HJ, et al. Diffusion-weighted MRI for unenhanced breast cancer screening. *Radiology* 2019;293:504-520.
33. He J, Shi H, Zhou Z, et al. Correlation between apparent diffusion coefficients and HER2 status in gastric cancers: Pilot study. *BMC Cancer* 2015;15:749.
34. Iqbal N, Iqbal N. Human epidermal growth factor receptor 2 (HER2) in cancers: Overexpression and therapeutic implications. *Mol Biol Int* 2014;2014:852748-852749.
35. Razek AA, Gaballa G, Denewer A, Nada N. Invasive ductal carcinoma: Correlation of apparent diffusion coefficient value with pathological prognostic factors. *NMR Biomed* 2010;23:619-623.
36. Sofi GN, Sofi JN, Nadeem R, et al. Estrogen receptor and progesterone receptor status in breast cancer in relation to age, histological grade, size of lesion and lymph node involvement. *Asian Pac J Cancer Prev* 2012;13:5047-5052.
37. Azizun N, Bhurgri Y, Raza F, Kayani N. Comparison of ER, PR and HER2/neu (C-erb B 2) reactivity pattern with histologic grade, tumor size and lymph node status in breast cancer. *Asian Pac J Cancer Prev* 2008;9:553-556.
38. Kim JY, Kim JJ, Hwangbo L, et al. Diffusion-weighted MRI of estrogen receptor-positive, HER2-negative, node-negative breast cancer: Association between intratumoral heterogeneity and recurrence risk. *Eur Radiol* 2020;30:66-76.
39. Ei Khoulil RH, Jacobs MA, Mezban SD, et al. Diffusion-weighted imaging improves the diagnostic accuracy of conventional 3.0-T breast MR imaging. *Radiology* 2010;256:64-73.